

Title No. 120-S33

Transition between Shear and Punching in Reinforced Concrete Slabs: Review and Predictions with ACI Code Expressions

by Alex M. D. de Sousa, Eva O. L. Lantsoght, and Mounir K. El Debs

One-way slabs under concentrated loads may fail by one-way shear, two-way shear, flexure, or a combination of these modes. This paper reviews shear and punching shear-failure mechanisms of one-way slabs under concentrated loads tested from the literature and investigates the accuracy of different approaches to predict the ultimate capacity for such slabs using the ACI code expressions. A database with 160 test results was evaluated. Shear and concentrated loads measured at failure were reviewed according to parameters such as the load position, slab width, and reinforcement ratios. The load position and slab width play a marked influence on the failure mechanism and tested loads. The analyses improved the understanding of the main parameters influencing the behavior of one-way slabs under concentrated loads. Finally, the proposed effective shear width expression enables accurate shear capacity predictions using the ACI code expressions.

Keywords: one-way shear; one-way slabs; punching shear; slabs under concentrated loads; transitional shear failure modes.

INTRODUCTION

One-way slabs under concentrated loads can develop a transitional failure mode between one-way shear, two-way shear, and flexure.¹ This loading is typical in solid slab bridges² and garage floors,³ but may also occur in floor slabs with heavy concentrated loads arising from building or industrial equipment.^{4,5} Without shear reinforcement, these slabs may develop a brittle failure mechanism, which is the most dangerous failure mode for these structures because it provides limited warning signs and does not allow safe user evacuation. Because most design codes do not provide specific recommendations to evaluate the shear and punching capacity of one-way slabs under concentrated loads, research in this field is necessary to guide designers.

Traditionally, most publications deal with the one-way shear capacity of beams or slabs loaded over the entire width^{6,7} (linear shear flow towards the support: Fig. 1(a)) or with the punching capacity of the slab-column connections of two-way slabs (radial shear flow around the load: Fig. 1(b)).⁸ However, the shear flow tends to be radial close to the load and linear close to the support⁹ when a concentrated load is placed close to line supports (Fig. 1(c); this figure uses the cracking pattern of different test results from Reifßen¹⁰). This behavior results in the possibility of varying shear failure mechanisms taking place. Figure 1(c) shows that a simply supported slab may develop a one-way shear failure or wide beam shear failure close to the line support,

as well as a punching failure around the concentrated load due to the characteristics of the shear flow in both regions.

Traditional approaches to evaluate the punching and shear capacity for such slabs are depicted in Fig. 2.^{1,11,12} Basically, the punching capacity is verified around the concentrated load, assuming a uniform shear force distribution around the critical perimeter (Fig. 2(a)). In the critical perimeter with two sides, it is assumed that the shear stresses develop only in the spanning direction on both sides of the load (Fig. 2(b.1)). For eccentric loads over the slab width, the free edges will limit the contribution of the sides of the critical perimeter near the border. Consequently, the decisive critical perimeter usually assumes three sides around the load contributing to the punching capacity (Fig. 2(b.2)). In the design and assessment of existing structures,¹³ as a rule of thumb, the smallest possible critical perimeter is used as it leads to the lowest capacity.¹⁴

The one-way shear capacity of slabs is commonly verified by assuming that only a slab strip b_{eff} contributes effectively to the shear capacity (Fig. 2(c)) with a uniform shear demand along this length, usually called the effective shear width. The most conventional approach to define the slab strip width contributing to the one-way shear capacity is based on an assumed horizontal load spreading from the far edge of the concentrated load to the support under a 45-degree angle,^{2,5,11} commonly named the French effective shear width,¹⁴ as it originates from France (Fig. 2(c)).

Previous studies addressed the accuracy level of analytical shear provisions to predict the shear^{11,15,16} and punching shear capacities^{11,16} of one-way slabs under concentrated loads. Lantsoght et al.,¹¹ for instance, evaluated 118 one-way slabs and wide beams (after filtering) with the European shear and punching shear code expressions.¹⁷ The comparison between experimental and predicted shear capacities showed a large scatter between tests and theoretical predictions, with many unsafe predictions. These results mainly occurred because the code expressions and rules of practice were applied without considering that, for example, the punching mechanism could be critical for the tests being evaluated by one-way shear expressions. In the same way,

ACI Structural Journal, V. 120, No. 2, March 2023.

MS No. S-2021-499.R2, doi: 10.14359/51738350, received August 4, 2022, and reviewed under Institute publication policies. Copyright © 2023, American Concrete Institute. All rights reserved, including the making of copies unless permission is obtained from the copyright proprietors. Pertinent discussion including author's closure, if any, will be published ten months from this journal's date if the discussion is received within four months of the paper's print publication.

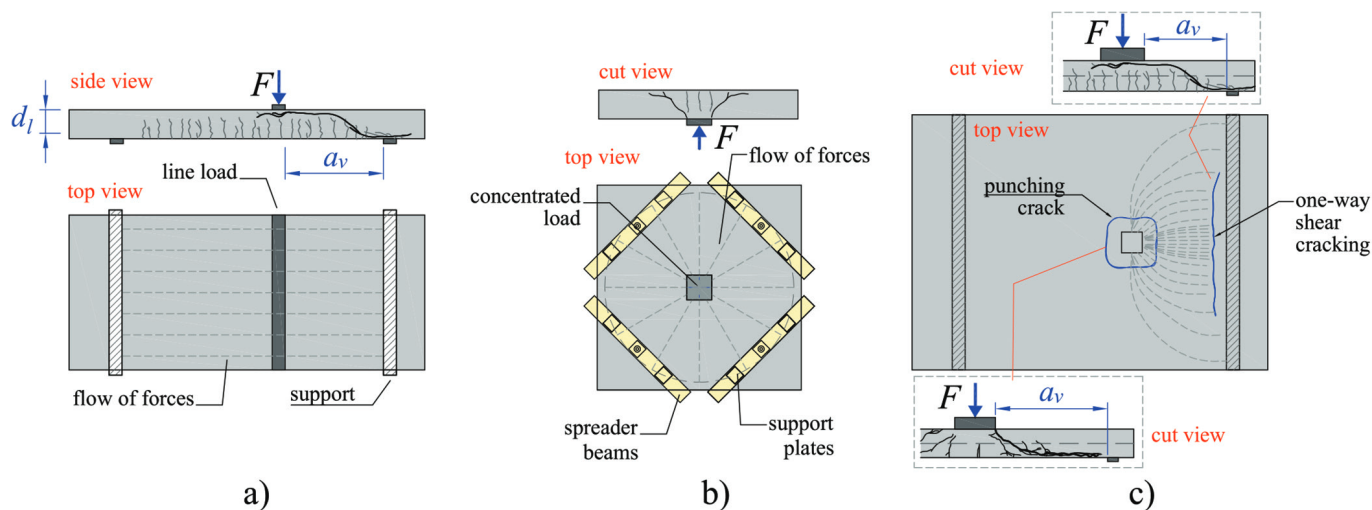


Fig. 1—Sketches of imaginary tests with expected cracking pattern and shear flow for: (a) beams and slabs loaded over entire width; (b) slab-column connections under concentric loads; and (c) one-way slabs under concentrated loads close to line support (shear flow to far support was omitted in sketch).

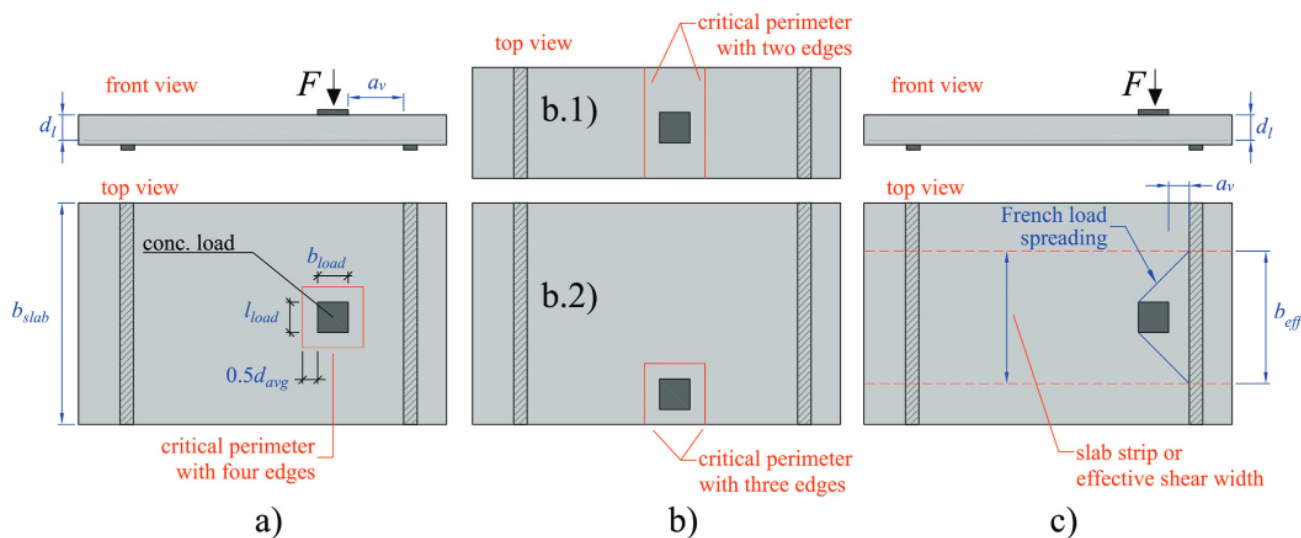


Fig. 2—(a) Most traditional critical perimeter definition for punching shear analyses; (b) possible critical perimeter for slabs with small width (b.1) and eccentric load over slab width (b.2); and (c) effective shear width b_{eff} defined to assess one-way shear capacity using French load spreading.¹⁴

the predictions of punching capacity did not fit well for the tests that failed as wide beams. Therefore, adjustments in the one-way shear and punching shear expressions should be made to account for these cases when using design code expressions devised for members loaded over the entire width or for slabs under concentric loads.

This paper starts by reviewing the one-way and two-way shear mechanisms involved in the problem of one-way slabs under concentrated loads. Subsequently, the cracking pattern of slabs from different experimental programs is discussed in detail to highlight the most important influencing parameters in the transition from one-way shear failure to two-way shear failures. A database with 160 test results from the literature was organized. Compared to previous works,¹⁸ different support conditions and failure mechanisms were addressed. A parameter analysis with test results was conducted to show how some parameters influence the measured loads at failure and the governing failure

mechanism of the tests. Afterward, regression analyses were conducted to derive enhanced expressions of effective shear width and shear-resisting control perimeter that can be used with the ACI shear code expressions.

RESEARCH SIGNIFICANCE

This work contributes to understanding the failure mechanism of one-way slabs under concentrated loads, a case frequently classified as the transition between one-way and two-way shear failures of reinforced concrete (RC) slabs. Moreover, it presents a specific evaluation of the current shear and punching shear expressions from the ACI 318-19 code¹⁹ when applied for one-way slabs under concentrated loads. This research identifies the key parameters for the sectional shear or punching capacity of one-way slabs under concentrated loads. Besides, an approach to consider these parameters, resulting in improved predictions of the ultimate capacity, is presented.

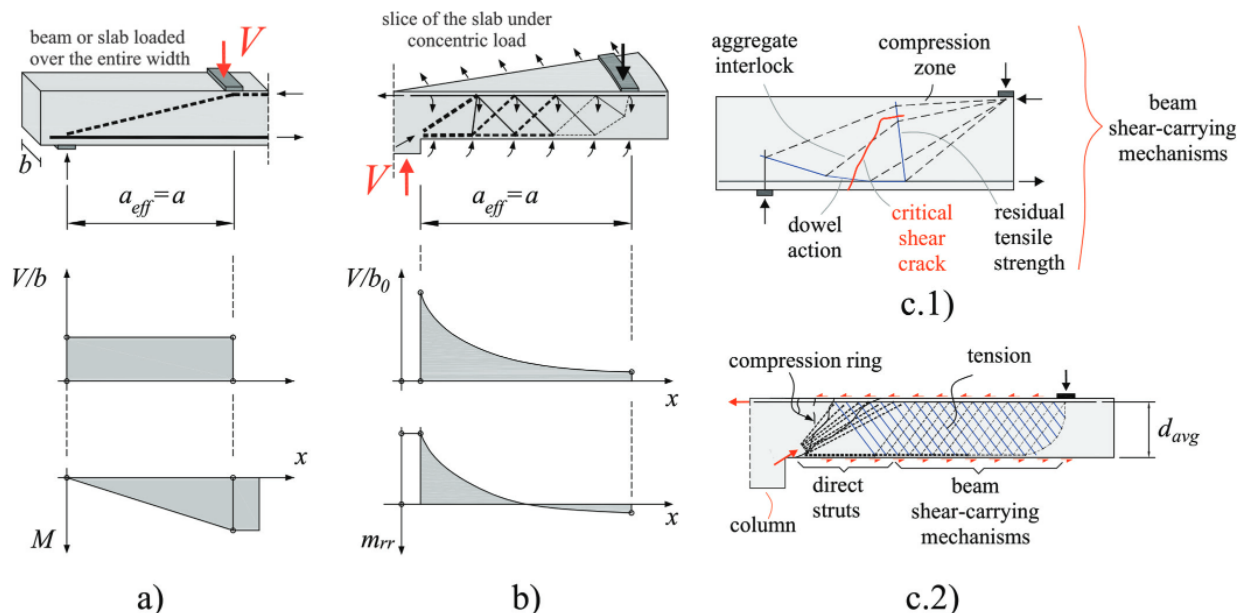


Fig. 3—Distribution of unitary shear forces and bending moments in the shear span for: (a) beams and slabs loaded over entire width; (b) slabs under concentric concentrated loads; (c.1) beam-shear carrying mechanisms of slender beams; and (c.2) direct struts and beam-shear carrying mechanisms of slabs under concentric loads. (Adapted from Muttoni and Fernandez Ruiz²⁶ and Cavagnis et al.²⁸)

LITERATURE REVIEW

Background of one-way shear and two-way shear-failure mechanisms

There are similarities and distinctions between one-way shear and two-way shear of slabs without shear reinforcement.¹ The main similarities include the shear-transfer mechanisms involved: i) compression chord capacity²⁰; ii) aggregate interlock²¹; iii) dowel action²²; iv) the residual tensile strength of concrete²³; and v) arching action or strut action.²⁴ According to the Critical Shear Crack Theory,^{8,25} the failure criteria for both one-way and two-way shear are governed by strain localization (flexure action), size effect (member thickness), and aggregate interlock effects²⁶ (roughness of the cracked surface). In the multi-action shear model from Marí et al.,²⁷ on the other hand, both one-way and two-way shear are governed by the compression chord capacity. In addition, these authors consider that both one-way and two-way shear failures occur when the inclined crack from flexure crosses the compression chord.

The main distinctions between one-way and two-way shear failures relate to the mechanisms that trigger the shear failures and the governing parameters of the crack kinematics: i) opening; and ii) sliding of the critical shear crack.²⁶ For instance, the opening of the critical shear crack is related to strains at the control section in one-way shear²⁵ and is related to slab rotations for two-way shear.⁸ Moreover, the relation between the applied load and the opening of the critical shear crack is almost linear for one-way shear but strongly non-linear for two-way shear.²⁶

Figure 3(a) shows that the distribution of unitary shear forces along the shear span is almost constant for beams and slabs loaded over the entire width (neglecting the influence of the self-weight).²⁶ However, a different behavior occurs in slabs under concentric loads (Fig. 3(b)). Because slabs transfer shear radially, a strong gradient of shear stresses

(shear force per unit length, with b_0 being the critical perimeter length around the loaded area) and bending moments takes place around the concentrated loads. Consequently, higher values of shear stresses arise near the concentrated load with significant strain localization in this region, which governs the punching capacity²⁶ (Fig. 3(b)).

Lantsoght et al.¹ also pointed out other differences: i) for punching, the inclined crack locations always arise immediately adjacent to the concentrated load, while for one-way shear in beams, the inclined crack is free to develop at the weakest section in the shear span a , closer to the support or to the load²⁹; and ii) although the inclined cracks may develop at similar shear stresses for beams and slabs, the opening of the critical shear crack for punching occurs only after a marked decrease of the tangential stiffness.³⁰ Marí et al.²⁷ also remarked that the critical punching crack follows an almost straight path due to the higher confining stresses generated around the column of flat slabs (compression ring). The inclination of the punching cracks is commonly related to the ratio between the failure load and the slab flexural capacity.³¹ Conversely, in one-way shear, the development of two main branches can be observed³²: an initial flexural crack and an inclined crack crossing the compression chord (Fig. 3(c.1)).

Another link between one-way and punching shear occurs on slab-column connections.²⁶ The larger shear transfer surface makes the shear forces moderate at large distances from the columns. Hence, the beam-shear carrying mechanisms from slender beams (shear transfer mechanisms i to iv) may provide the required punching capacity (Fig. 3(c.1)). However, close to the concentrated load, a small perimeter carries the shear forces and arching action develops, increasing the unitary shear strength in this region (Fig. 3(c.2)). As a result, the unitary shear strength for punching shear (when the critical perimeter is consistently

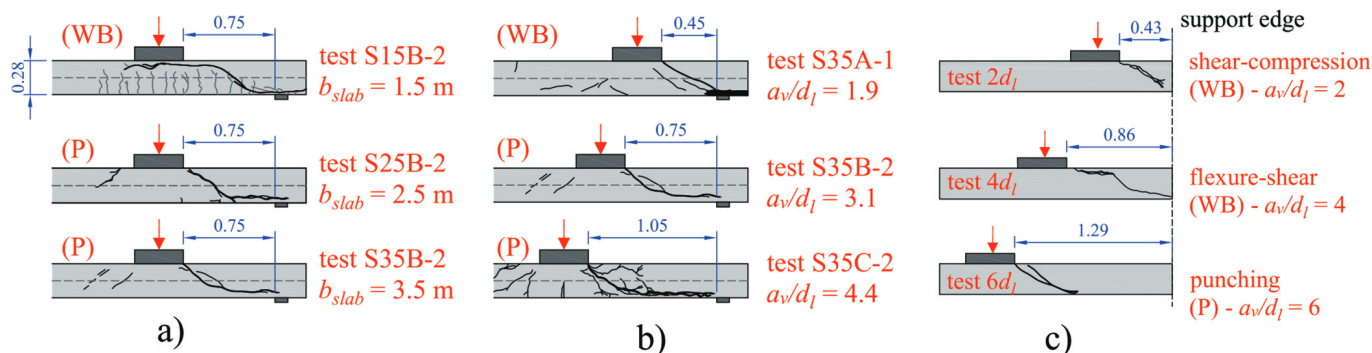


Fig. 4—Transition of shear-failure mechanisms as function of: (a) slab width; (b) shear slenderness a_v/d_l for simply supported slabs from Reißen et al.³⁵; and (c) shear slenderness a_v/d_l for cantilever slabs for tests from Henze.³⁸ (Note: 1 m = 3.3 ft.)

placed closer to the concentrated load) is higher than that for one-way shear.²⁶

Effect of slab width-load size ratio b_{slab}/l_{load}

A limited number of studies focus on explaining the transition from one-way to two-way shear failures,^{1,33} even though some experimental programs reported different shear failure mechanisms in the tests of slabs under asymmetrical concentrated loads.^{2,34,35}

Reißen et al.³⁵ and Lantsoght et al.³⁶ identified experimentally that the one-way shear capacity V_{test} of slabs under concentrated loads does not increase linearly by increasing the slab width b_{slab} or the ratio b_{slab}/l_{load} , where l_{load} is the width of the loading plate in the transverse direction. Therefore, these results are consistent with the concept of using an effective shear width for wide members under one-way shear (Fig. 2(c)). In addition, it was also demonstrated experimentally that the failure load (P_{test}) decreases by decreasing the slab width b_{slab} or the ratio b_{slab}/l_{load} .³⁵ This occurs because slabs with a smaller width develop a more unidirectional shear flow to the support, which decreases the load distribution in the transverse direction. Previous studies³⁷ also showed through linear elastic finite element analyses that as b_{slab} increases, the gradient of bending moments around the concentrated load increases, which favors the occurrence of punching failures over one-way shear failures for wider slabs.

Saw cuts of failed specimens can be used to identify the transition of shear failure mechanisms. Figure 4(a) shows the cracking pattern of a set of slabs tested by Reißen et al.,³⁵ where the only parameter varied was the slab width (b_{slab}): 1.5, 2.5, and 3.5 m (4.92, 8.20, and 11.48 ft). The loading arrangement was similar to that shown in Fig. 2(a). The concentrated load was applied on a square area with a size of 0.40 x 0.40 m (1.31 x 1.31 ft) with $a = 1$ m (3.28 ft), with a being the center-to-center distance between the load and the support. Figure 4(a) shows that the governing shear failure mechanism changed from wide beam shear (WB) to punching shear (P) as b_{slab} increased. Test S15B-2 developed a critical shear crack typical for one-way shear, based on the visible flexure cracks and the horizontal branch of the critical shear crack crossing the compression chord. At the same time, S35B-2 developed a critical shear crack without the horizontal branch at the compression chord and with the inclined branch of the critical shear crack reaching the edges

of the loaded area, as is common for punching failures. In S25B-2 and S35B-2, the critical shear crack was more pronounced in the region with the largest shear demand—that is, in the shear span—and the full punching cone did not develop.

Effect of shear slenderness a_v/d_l

One of the consequences of using an effective width, as sketched in Fig. 2(c), is that the predicted one-way shear capacity increases with the shear slenderness a_v/d_l (d_l is the effective depth toward longitudinal steel and a_v is the clear shear span—the distance between the edge of support and edge of the load). However, some studies showed that when increasing a_v/d_l —from 1 to 6 in Henze et al.³⁴ and from 1.9 to 4.4 in Reißen et al.³⁵—and keeping all other parameters constant, the tested one-way shear capacity of the slabs decreased markedly or remained almost the same after a certain value of a_v/d_l . At the same time, Lantsoght et al.² showed that decreasing the ratio a_v/d_l from 1.70 to 0.75 increased the failure loads substantially, even though the calculated effective shear width decreased, which they explained by the formation of a fan of compressive struts between the load and the support. However, the resistance increase due to the arching action was less pronounced in the slab members than in beams² due to the fan of struts and their resulting load path with varying a_v/d_l . Therefore, the increase of arching action was also a function of the slab width.³⁶

Figure 4(b) shows the same governing shear failure mechanism change as the shear slenderness a_v/d_l increases. Note that S35A ($a_v/d_l = 1.9$) indicates a shear-compression failure as typical in non-slender beams (inclined critical shear crack between the load and the support without major flexure cracks in the shear span). Figure 4(c) shows the cracking pattern of cantilever slabs with $b_{slab} = 4.5$ m (14.76 ft) and cantilever length 1.9 m (6.23 ft) tested by Henze³⁸ as a function of a_v/d_l . Figure 4(c) shows the same transition from one-way to punching shear failures as the shear slenderness a_v/d_l increased for cantilever slabs.

Effect of transverse reinforcement ratio ρ_t

The reinforcement ratio in the transverse direction of slabs (perpendicular to the shear span) also influences the governing shear failure mechanism of slabs under concentrated loads. Lantsoght et al.² observed that higher

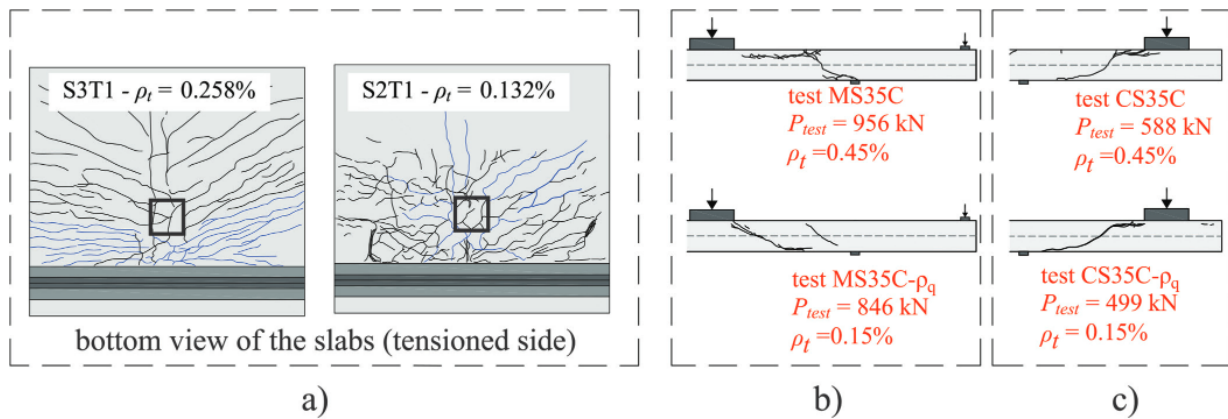


Fig. 5—Effect of transverse reinforcement ratio ρ_t on shear/punching capacity and governing failure mechanism for slabs with: (a) load applied close to simple supports (figures adapted from Lantsoght et al.²); (b) load applied close to continuous support; and (c) load applied on cantilever slabs (figures adapted from Reifßen¹⁰). (Note: 1 kN = 0.225 kip.)

transversal reinforcement ratios led to a better force distribution in the width direction because the cracking pattern in the shear span was more similar to that of one-way slabs loaded over the entire width. Instead, slabs with lower transverse reinforcement ratios developed a cracking pattern that was more localized (radial and tangential cracks) around the concentrated load, similar to that of a punching failure (Fig. 5(a)). When the transverse and longitudinal reinforcement ratios are different, the unitary shear capacities around the concentrated load are different.^{39,40} Because the distribution of shear forces around the load is also uneven⁴¹ and depends on the load position and boundary conditions, failure can be triggered in the region of higher demand or lower resistance.

A similar change in the shear failure mechanism was observed in the continuous slabs tested by Reifßen et al.,³⁵ where the cracking pattern in cut views of the tests MS35C ($\rho_t = 0.45\%$) and MS35C- ρ_q ($\rho_t = 0.15\%$) indicated that the slab with a lower transverse reinforcement ratio failed in punching shear (Fig. 5(b)), while the other one failed by one-way shear. The change in the externally applied load at failure P_{test} was only 13% between these two tests.

On the other hand, decreasing ρ_t had a more limited effect on the cracking pattern and governing shear failure mechanisms for cantilever slabs. Figure 5(c) shows that decreasing ρ_t from 0.45 to 0.15% for cantilever slabs decreased the failure load (P_{test}) by 18% and resulted in almost no change in the cracking pattern in the cut views.

DATABASE

The references gathered in the database and the range/distribution of parameters are presented in Appendix A.* This study: i) reviews the test results from the literature in a comprehensive way (including failure mechanisms, cracking pattern, and ultimate loads); and ii) presents an enhanced approach to predict the ultimate capacity of slabs under concentrated loads that failed by one-way shear as wide beams (WB), by punching shear (P) and a mixed

failure mode between one-way shear and punching shear (WB+P). Only tests with $b_{slab}/d_l > 5$ were considered. The criteria of using only tests with ratio $(b_{slab} - l_{load}) > 4d_{avg}$ was also included as a filter to remove tests with predominant one-way shear behavior. This filter increases the proportion of tests that could present both shear failure mechanisms at failure. In practice, all tests that do not satisfy this criterion failed as wide beams in one-way shear and could introduce a slight bias in the statistical analyses.

In total, Database A includes the results from 160 tests under different support conditions: i) 77 tests with a load close to a simple support (SS); ii) 20 tests with a load close to a continuous support (CS); and iii) 46 tests with the load applied on a cantilever slab (CT). Database A is available in the public domain⁴² and is inspired by previous databases of slabs under concentrated loads failing in shear and punching shear.^{10,11} This database was used mainly to perform parameter analyses of selected parameters in the tested sectional shear V_{test} and concentrated loads at failure P_{test} . To evaluate the effect of selected parameters, such as the clear shear slenderness a_v/d_l , groups of test results where only a_v/d_l was varied were taken from Database A⁴² to analyze this effect further. In this way, different subsets were organized to evaluate each parameter selected.

- **Database A1** brings together test results for which the main parameter varied was the shear slenderness a_v/d_l (75 test results from the following references: Natário,⁴¹ Reifßen,¹⁰ Rombach and Henze,⁴³ Lantsoght,¹⁴ Cullington et al.,⁴⁴ Ferreira,⁴⁵ and Regan¹²).
- **Database A2** brings together test results for which the main parameter varied was the slab width to load size ratio b_{slab}/l_{load} (26 tests from the following references: Reifßen,¹⁰ Lantsoght,¹⁴ and Regan and Rezai-Jarobi⁴⁶).
- **Database A3** brings together test results for which the main parameter varied was the transverse reinforcement ratio ρ_t (36 tests from the following references: Damasceno,⁴⁷ Ferreira,⁴⁵ Reifßen,¹⁰ and Lantsoght¹⁴). The analyses related to this dataset are presented in Appendix B, because the influence of this parameter was considered secondary in this study.

Database B is also a subgroup of Database A but received a different classification as this database was used to evaluate

*The Appendix is available at www.concrete.org/publications in PDF format, appended to the online version of the published paper. It is also available in hard copy from ACI headquarters for a fee equal to the cost of reproduction plus handling at the time of the request.

the performance of shear and punching capacity predictions with the ACI 318-19 code expressions. In Database B, tests that developed flexure-induced punching (F+P) at failure were removed. This database contains 143 test results of one-way slabs under concentrated loads: i) 40 tests failed by punching (P); ii) 91 tests failed as wide beams by one-way shear mechanisms (WB); and iii) 12 tests failed by a mixed-mode between one-way shear and two-way shear (WB+P).

PARAMETER ANALYSES ON GOVERNING SHEAR-FAILURE MODE

This section evaluates the influence of parameters such as the load position a_v (or shear slenderness a_v/d_l) and slab width to load size ratio b_{slab}/l_{load} on the sectional shear and concentrated loads applied at failure for one-way slabs under concentrated loads, as well as on the transition between these shear failure modes. For this purpose, different subgroups of Database A were used.

In this study, it is assumed that the full one-way shear capacity may not have been reached in the tests that failed by punching ($V_{test} < V_{exp}$) and, in the same way, the full punching capacity may not have been reached in the tests that failed as wide beams in one-way shear ($P_{test} < P_{exp}$). Because of this, in the following analyses, the shear (V_{Fu}) and punching capacities (P_{test}) refer respectively to: i) the corresponding sectional shear forces at failure due to the concentrated load; and ii) the maximum concentrated loads measured on the tests. In this text, V_{test} is the total sectional shear measured at failure, including the self-weight influence along the entire slab width

$$V_{test} = V_{Fu} + v_g \cdot b_{slab} \quad (1)$$

where v_g is the shear force per unit length due to the self-weight at the section $a/2$; and V_{Fu} is the sectional shear considering only the applied load F_u at failure. As suggested by Reißer,¹⁰ this study uses V_{Fu} instead of V_{test} to not include the influence of the effective shear width assumed in the calculation of V_{test} .

Some analyses were inspired by the research from Reißer,¹⁰ who investigated the influence of similar parameters on the one-way shear capacity of slabs under concentrated loads (sectional shear reached in the tests V_{Fu}). However, to allow a broader insight into different shear failure mechanisms, both sectional shear and concentrated loads applied at failure are addressed in this study. Moreover, the governing failure mechanism is highlighted on all graphs to identify the transition between the failure mechanisms according to the parameters investigated. Therefore, these analyses provide a new look at the problem.

The influence of the concrete compressive strength was reduced by normalizing the sectional shear and externally applied load at failure (V_{Fu} and P_{test}) to the square root of the concrete compressive strength $\sqrt{f_c}$, such as recommended in de Sousa et al.⁶ and in line with the one-way and two-way shear expressions from the ACI 318-19 code¹⁹ (f_c is the average compressive strength of concrete measured on cylinder specimens). Additionally, the sectional shear and externally applied load at failure (V_{Fu} and P_{test}) were also

normalized to the effective depth d_l . Therefore, the ratio $V_{Fu}/d_l \cdot \sqrt{f_c}$ is a measure of the tested shear capacity on which the effect from the concrete compressive strength and the effective depth was removed to compare different experimental programs better.

Shear slenderness a_v/d_l

The shear slenderness a_v/d_l is a well-known parameter influencing the shear capacity of beams and wide members loaded over the entire width.⁶ For ratios $a_v/d_l < 2$, the shear capacity of RC beams without stirrups is enhanced as a result of arching action between the load and the support. Figure 6 shows the relation between the normalized shear V_{Fu} and concentrated load at failure P_{test} as a function of a_v/d_l to the Database A1. Lines connect tests in which only the ratio a_v/d_l was varied. The symbols identify the governing failure mechanism based on the cracking pattern and reported information from the original references.

Figure 6(a) shows that both shear and punching failures were observed for tests with $a_v/d_l < 3$. On the other hand, all tests with $a_v/d_l > 5$ failed by punching (P) or a mixed mode between shear and punching (P or WB+P). The tests on which a punching failure occurred with $a_v/d_l < 3$ are mainly slabs with thickness $h < 125$ mm (4.92 in.). Therefore, the governing failure mechanism also seems to be influenced by the absolute slab thickness, in addition to the ratio a_v/d_l .

As already pointed out by Reißer,¹⁰ an increase in the effective shear width with the shear slenderness cannot be confirmed based on Fig. 6(a). Contrarily, the normalized sectional shear at failure (regardless of governing failure mechanism identified) seems to decrease for most tests as a_v/d_l increases.

In this study, the normalized failure load P_{test} was also evaluated in detail (Fig. 6(b)). The highlights in green indicate sets of tests on which an increase of a_v/d_l resulted in an increase of P_{test} . In other words, it was identified that, although the measured sectional shear V_{Fu} decreased for most tests (Fig. 6(a)), the failure load P_{test} increased for some tests. Notably, for the cases where the failure load P_{test} increased for an increasing ratio of a_v/d_l , the test with a higher ratio of a_v/d_l failed in punching (Fig. 6(b)—data points in blue). Therefore, tests critical for punching may benefit from the less-uneven distribution of shear forces around the load when the shear slenderness increases. Tests critical in one-way shear commonly fail at a lower concentrated load when the shear slenderness increases.

In this study, the increase of the failure loads P_{test} by increasing the ratio a_v/d_l may be better explained by looking at the ratio a/l_{span} . Loads applied at the slab center have an $a/l_{span} = 0.5$ and no shear demand difference between the front and back faces of the critical perimeter. Tests with lower a_v/d_l have a $0 < a/l_{span} < 0.5$ and a higher difference between the shear demand at the front and back faces of the critical perimeter, also called non-proportional loading of the punching perimeter. In other words, the tests with higher a_v/d_l —and hence, higher a/l_{span} —benefit from the most balanced shear demand around the critical perimeter. Tests with lower a_v/d_l fail when the most heavily loaded sides of the critical perimeter (between the front and back faces of

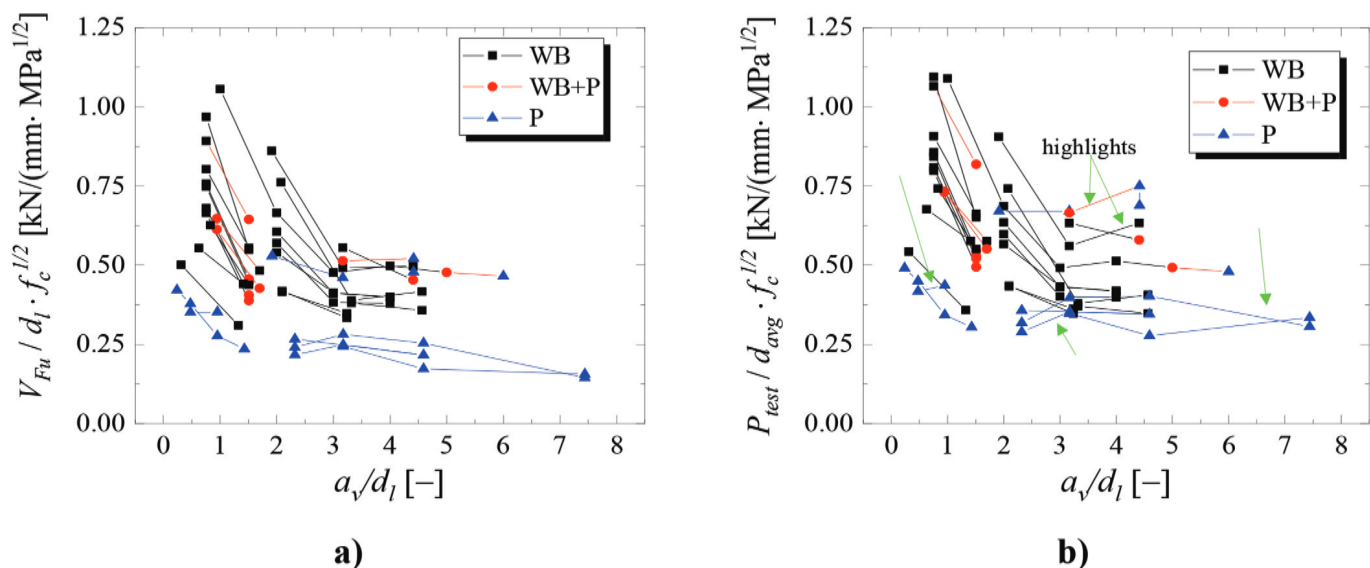


Fig. 6—Influence of shear slenderness a_v/d_l on normalized: (a) sectional shear; and (b) failure loads for one-way slabs under concentrated loads using Database A1 with 75 test results.

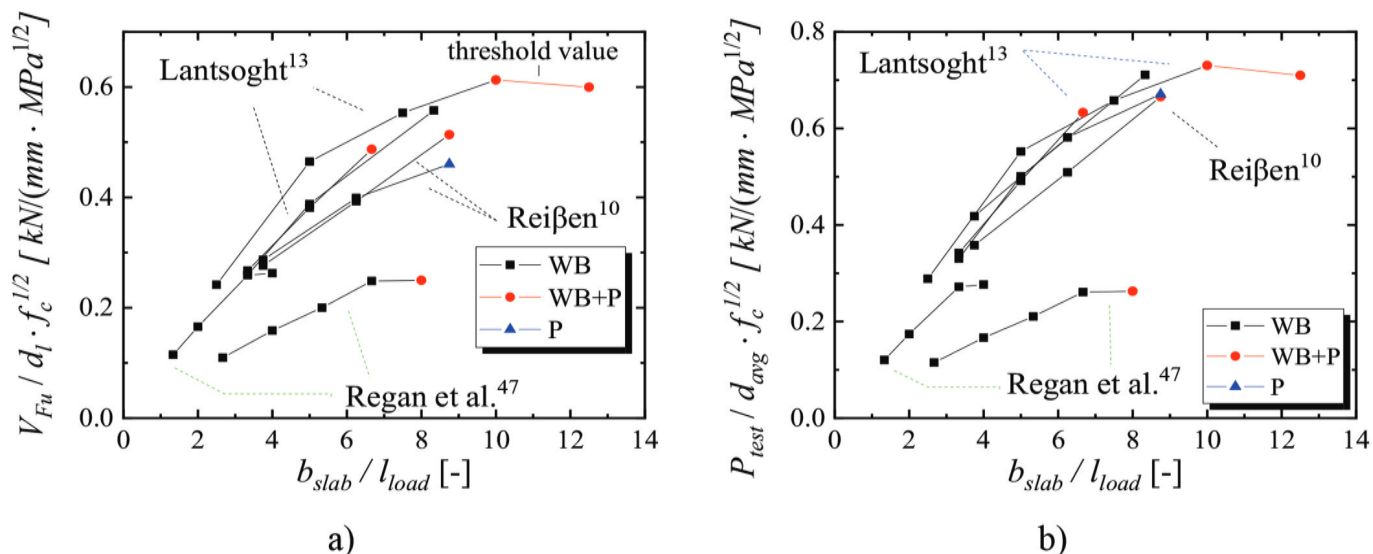


Fig. 7—Influence of slab width-load size ratio b_{slab}/l_{load} on: (a) sectional shear; and (b) failure load of slabs under concentrated loads from Database A2. (Note: 1 kN = 0.225 kip; 1 MPa = 145 psi; 1 mm = 0.0394 in.)

the load) reach their full capacity. In the tests S35B-2 from Reißer¹⁰ (Fig. 4), for instance, the critical shear crack is visibly more clearly at the front face of the load, indicating that failure started at the front face.

Slab width-load size ratio b_{slab}/l_{load}

Figure 7 shows how the ratio of b_{slab}/l_{load} influences the sectional shear (Fig. 7(a)) and failure load (Fig. 7(b)) of one-way slabs under concentrated loads from Database A2. Figure 7 shows that the sectional shear at failure increases until a certain threshold when the ratio b_{slab}/l_{load} is increased (by increasing the width of the tested specimen). In the tests from Regan and Rezai-Jorabi⁴⁶ and from Lantsoght,¹⁴ the threshold value occurred when the slabs started to fail by punching instead of by one-way shear. In the tests from Reißer,¹⁰ a change in the rate of increase of sectional shear (change in slope of lines) was observed when the failure

mode changed from one-way shear to punching shear or a mixed failure mode.

These findings are in line with Lantsoght et al.³⁶ and Reißer,¹⁰ who observed that by increasing the slab width until a certain value, the shear capacity does not increase anymore, meaning that the effective contributing width to the sectional shear capacity has an upper limit. It can also be noted that the sectional shear at failure increased almost linearly with b_{slab}/l_{load} for the three experimental programs until a certain point. Notably, the threshold value for the tests from Regan and Rezai-Jorabi⁴⁶ was reached for a smaller value of b_{slab}/l_{load} compared to the tests from Lantsoght¹⁴ and Reißer.¹⁰ This occurs because the slabs tested by Regan and Rezai-Jorabi⁴⁶ had a considerably lower thickness than those tested by the other authors ($d_l = 83$ mm [3.24 in.] compared to $d_l = 265$ mm [10.34 in.] on average). Therefore, it can be concluded that the transition from one-way shear failures to

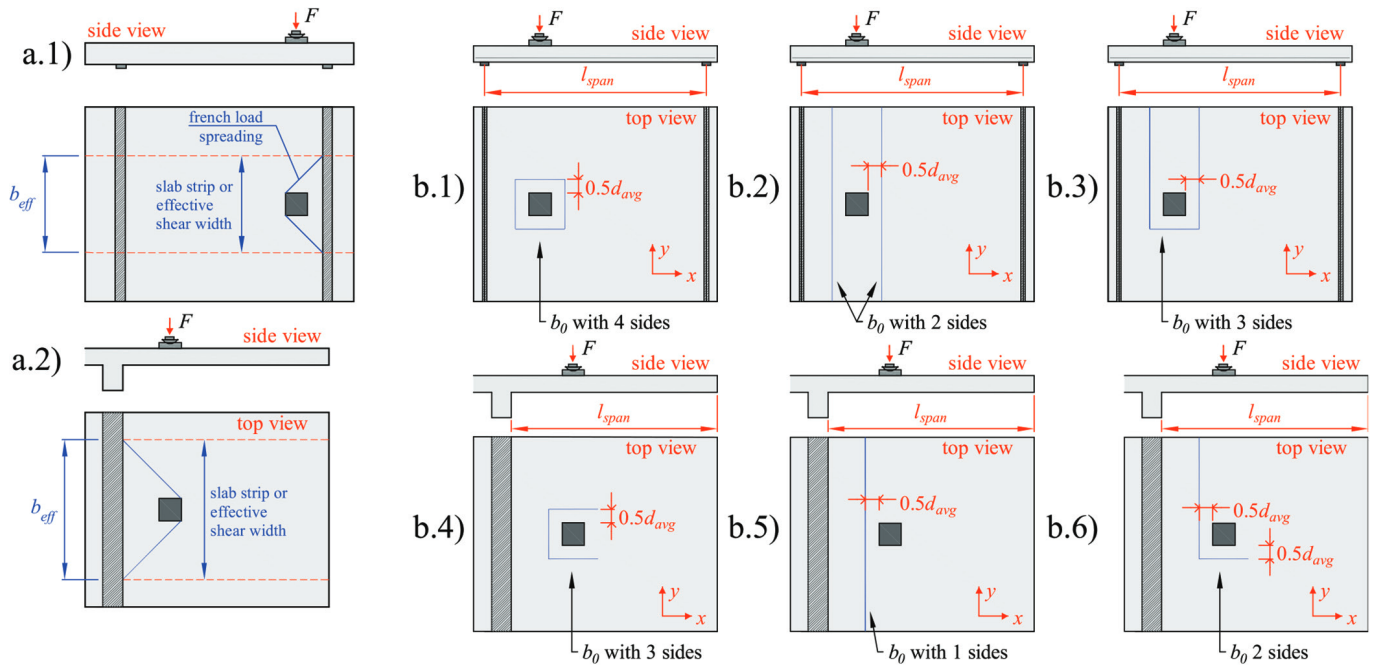


Fig. 8—(a) Definition of slab strip or effective shear width b_{eff} that contributes to sectional shear capacity V_c based on literature review for: (a.1) simply supported and continuous slabs and (a.2) cantilever slabs; and (b) definition of possible control perimeters depending on load position and slab geometry for: (b.1), (b.2), and (b.3) simply supported and continuous slabs; (b.4), (b.5), and (b.6) cantilever slabs.

punching failures does not depend exclusively on b_{slab}/l_{load} , but also on the slab thickness.

EVALUATION WITH ACI SHEAR AND PUNCHING SHEAR PROVISIONS

The code provisions from ACI 318-19¹⁹ for one-way and two-way shear (punching) were modified in the last revision.^{19,48,49} Equations (2) to (4) depict the current expressions used to evaluate the nominal shear and punching resistances of reinforced concrete members without shear reinforcement (that is, shear stress per unit area along the control section or control perimeter). Between the main modifications: i) the size effect parameter λ_s was included in both shear and punching expressions; and ii) the longitudinal reinforcement ratio ρ_l was directly considered in the one-way shear equations^{48,49} (equations in SI units; f'_c in MPa; d_l , d_{avg} , and b_0 in mm).

$$v_{c,shear} = \min \left\{ \begin{aligned} &0.66 \cdot \lambda_s \cdot \lambda \cdot \rho_l^{1/3} \cdot \sqrt{f'_c} + \frac{N_u}{6 \cdot A_g} \\ &0.29 \cdot \sqrt{f'_c} \end{aligned} \right. \quad (2)$$

$$\lambda_s = \sqrt{\frac{2}{1 + 0.004 \cdot d_l}} \leq 1 \quad (3)$$

$$v_{c,punch} = \min \left\{ \begin{aligned} &0.33 \cdot \lambda_s \cdot \lambda \cdot \sqrt{f'_c} \\ &0.17 \cdot \left(1 + \frac{2}{\beta_{rect}} \right) \cdot \lambda_s \cdot \lambda \cdot \sqrt{f'_c} \\ &0.083 \cdot \left(2 + \frac{\alpha_s \cdot d_{avg}}{b_0} \right) \cdot \lambda_s \cdot \lambda \cdot \sqrt{f'_c} \end{aligned} \right. \quad (4)$$

The one-way shear capacity of one-way slabs under concentrated loads is usually checked by assuming that a slab strip with a width equal to the effective shear width contributes to the sectional shear capacity V_c of the slab (Fig. 8(a)). The punching capacity P_c is usually checked by considering a control perimeter b_0 contributing to the punching resistance (Fig. 8(b)). Therefore, the shear and punching capacities are determined by

$$V_{c,predicted} = v_{c,shear} \cdot b_{eff} \cdot d_l \quad (5)$$

$$P_{c,predicted} = v_{c,punch} \cdot b_0 \cdot d_{avg} \quad (6)$$

For punching, the control perimeter b_0 used shall be the smallest, considering the different layouts possible. Figure 8(b) shows some possible configurations for the control perimeter for a given load position. In practice, depending on the load position with regard to the free edges, slab width, and boundary conditions, one or another layout will govern. For example, the control perimeter with two sides is commonly the smallest for simply supported slabs with a reduced slab width (Fig. 8(b.2)). For loads close to a free edge, the control perimeter with three sides usually governs (Fig. 8(b.3)).

This study evaluated a set of one-way slabs under concentrated loads, including 143 test results from the literature, with the ACI shear and punching shear expressions (Database B). The effective shear width (Fig. 8(a)) and control perimeter (Fig. 8(b)) required for such evaluations were defined according to previous recommendations and guidelines from the literature.^{2,50}

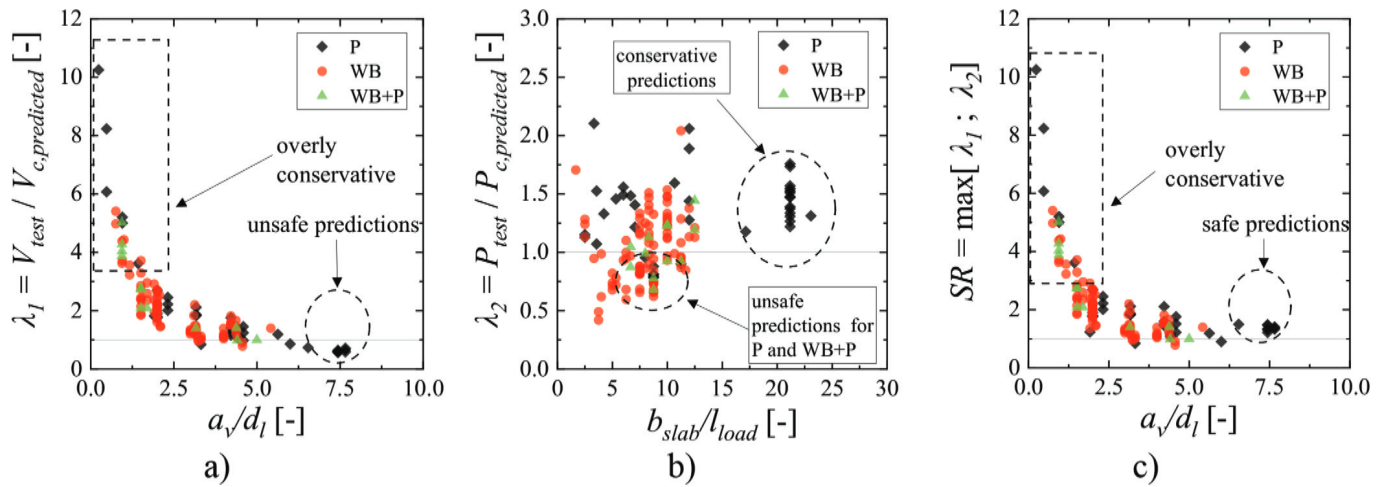


Fig. 9—Relation between tested and predicted resistances for one-way slabs under single concentrated loads using 143 test results that failed by different mechanisms: (a) one-way shear predictions; (b) punching capacity predictions; and (c) combining predictions of one-way shear and punching shear capacities.

Figure 9 shows that undesirable predictions were found for the shear and punching capacities predicted with the ACI 318-19 code expressions.¹⁹ In Fig. 9, V_{test} and P_{test} represent the achieved sectional shear and achieved applied load at failure. $V_{predicted}$ and $P_{predicted}$ represented the predicted sectional shear and predicted punching capacity with the ACI 318-19¹⁹ expressions. For instance, the one-way shear capacity predicted for the slabs tested with $a_v/d_l < 3$ could be overly conservative (Fig. 9(a)). Moreover, unsafe predictions of sectional shear capacity could be found in tests with $a_v/d_l > 5$, which typically failed by punching (Fig. 9(a)). When evaluating the punching capacity with the ACI 318-19¹⁹ expressions (Fig. 9(b)), the predictions for tests with large slab width compared to the load size ($b_{slab}/l_{load} > 12.5$) are satisfactory in safety and accuracy ($1 < P_{test}/P_{c,predicted} < 2.5$). However, for tests with $b_{slab}/l_{load} < 12.5$ that failed by punching (P) or a mixed mode between one-way shear and punching shear (WB+P), the predictions of punching capacity overestimated the tested capacity. This result is generally unsatisfactory because the punching expressions were devised to provide a conservative estimate of punching capacity (assuming reinforcement yielding at failure⁵¹). In practice, one-way shear and punching shear capacities must be evaluated together to determine the most critical applied load for a given slab ($F_{predicted}$). This means that the load $F_{predicted,shear}$ correlated to the sectional shear capacity $V_{predicted}$ needs to be compared to the load $F_{predicted,punching}$ correlated to the punching capacity $P_{predicted}$. This comparison can be easily made, as shown in Fig. 9, by defining a strength ratio $SR = \max(V_{test}/V_{predicted}, P_{test}/P_{predicted})$. This comparison helps define the most critical relation between tested and predicted resistances. The reader should note that most publications do not discuss this aspect of the problem. In summary, it is not a problem for design or assessment if the predictions of one-way shear capacity are unsafe if the predictions of punching capacity are governing (which means predicting a safer load capacity). However, Fig. 9(c) shows that despite being on the safe side, most predictions combining shear and punching predictions are overly conservative.

Therefore, there is a need for improved approaches, particularly for the sectional shear of one-way slabs based on the effect of parameters such as the shear slenderness a_v/d_l .

PROPOSED APPROACH FOR ONE-WAY SHEAR CAPACITY PREDICTIONS

Two coefficients are proposed to be combined with the one-way shear expression from ACI. These coefficients were derived based on statistical regression analyses and the observations performed in the literature review. The coefficient $\mu_{1,shear}$ is related to the improved shear capacities of members for concentrated loads close to the support, here assumed for distances $a_v < 2d_l$. This factor considers the enhanced shear capacities due to the formation of direct compressive struts transferring the load directly to the supports beyond the inclined crack formation^{2,36} (arching action). The improved shear capacities are accounted for by multiplying the unitary shear capacities $v_{c,shear}$ from ACI 318-19¹⁹ with the factor $\mu_{1,shear}$, as originally proposed by Regan⁵² and adopted in the European code¹⁷ and *fib* Model Code 2010⁵³

$$\mu_{1,shear} = 1/\beta_{arching} \quad (7)$$

$$\beta_{arching} = a_v / 2d_l; 0.25 \leq \beta_{arching} \leq 1$$

For loads close to the support in slabs (for instance, $a_v < 2d_l$), the one-way shear capacity could also be evaluated as the shear capacity of non-slender beams. For such cases, the ACI 318-19¹⁹ recommends using strut-and-tie models. However, three-dimensional models would be necessary for slabs under concentrated loads, which are not addressed in the code. Consequently, it is common to use the same equations devised for slender members to evaluate the one-way shear resistance of slabs.

The coefficient $\mu_{2,shear}$ has two functions: i) it increases the effective shear width b_{eff} when $a_v < 2d_l$ based on the enhanced horizontal load spreading of shear forces for loads close to the support; and ii) it decreases the predicted effective shear width ($b_{eff,prop}$) for loads farther away from the support. The latter was necessary to avoid unsafe capacity

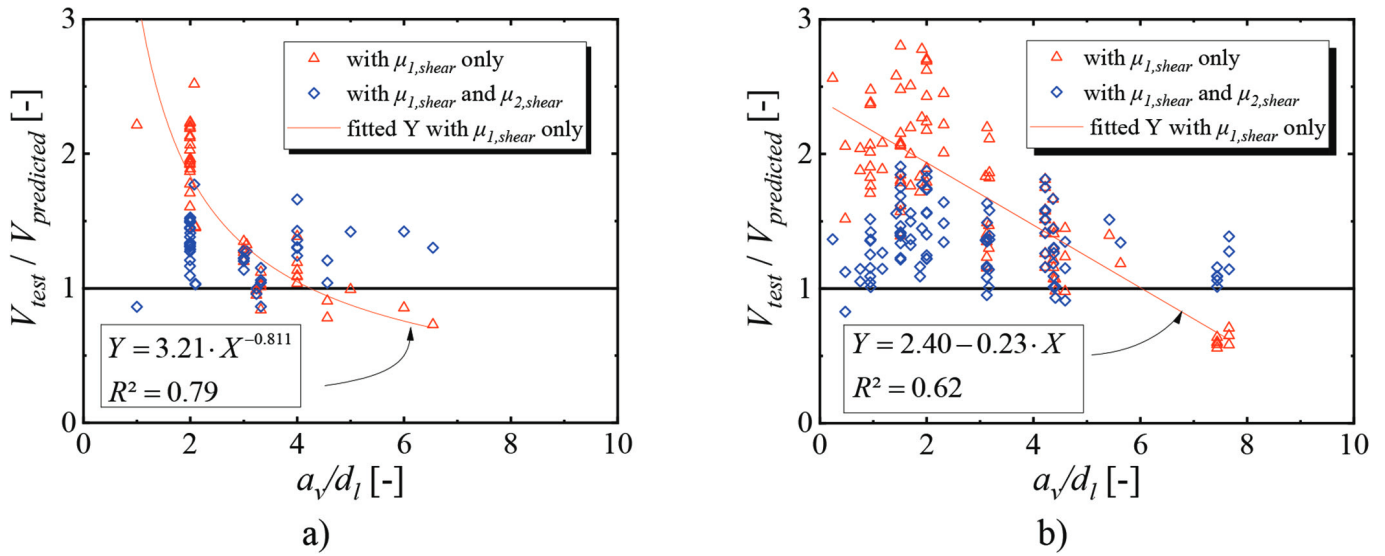


Fig. 10—Calibration of $\mu_{2,shear}$ for: (a) cantilever slabs; and (b) slabs with concentrated load close to simple or continuous support.

predictions for tests that may develop punching failure mechanisms.^{37,54} Figure 10 shows the linear and non-linear regression analyses performed to derive the coefficient $\mu_{2,shear}$ for different support conditions. Figure 10(a) represents the calibration of $\mu_{2,shear}$ for the cantilever slabs (46 test results from Database B), and Fig. 10(b) depicts the calibration of $\mu_{2,shear}$ for loads close to the simple or continuous support (97 test results from Database B).

Equations (8) and (9) give the semi-empirical factors $\mu_{1,shear}$ and $\mu_{2,shear}$ (dimensionless values) for the one-way shear expressions and $b_{eff,prop}$ (SS is simple support, CS is continuous support, and CT is cantilever support). These coefficients are simplified from the results of the regression analysis.

$$\mu_{2,shear} = 2.57 \cdot (a_v / d_l)^{-0.81} \begin{cases} \leq 2.57 \\ \geq 0.56 \end{cases}, \text{ for CT}; \quad (8)$$

$$\mu_{2,shear} = -0.18 \cdot (a_v / d_l) + 1.92 \begin{cases} \leq 1.88 \\ \geq 0.51 \end{cases}, \text{ for SS and CS}$$

$$b_{eff,prop} = b_{eff,french} \cdot \mu_{2,shear} \begin{cases} \leq b_{slab} \\ \geq l_{load} + 4 \cdot d_l \end{cases} \quad (9)$$

The sectional shear capacity using the proposed recommendations is given by

$$V_{c,proposed} = (v_{c,shear} \cdot \mu_{1,shear}) \cdot b_{eff,prop} \cdot d_l \quad (10)$$

PROPOSED APPROACH FOR PUNCHING CAPACITY PREDICTIONS

This study assumes that the punching capacity predictions for one-way slabs under concentrated loads should be based on simple expressions, similar to those provided in the current ACI 318-19.¹⁹ Based on the literature review and statistical analyses, two aspects should be considered when evaluating the punching capacity with the ACI code expressions: i) the enhanced nominal punching capacity in the

portion of the control perimeter closer to the support (front face of the load) as originally proposed by Regan¹³; and ii) the lower contribution of the lateral sides of the control perimeter (parallel to the free edges of the slabs) (refer to Fig. 11).

According to the proposed approach, the punching capacity can be estimated by the following expressions

$$P_{c,proposed} = (v_{c,punch,eff} \cdot \mu_{1,punch}) \cdot b_{0,x1} \cdot d_{avg} + v_{c,punch,eff} \cdot b_{0,x2} \cdot d_{avg} + 2 \cdot v_{c,punch} \cdot (b_{0,y} \cdot \mu_{2,punch}) \cdot d_{avg} \quad (11)$$

The contribution of the side $b_{0,x2}$ can be neglected for cantilever slabs (Fig. 11(c)). The factor $\mu_{1,punch}$ is equal to $\mu_{1,shear}$. The factor $\mu_{2,punch}$ is derived based on statistical analyses and simplified to

$$\mu_{2,punch} = 2.72 \cdot 10^{-4} \cdot (b_{slab} / l_{load})^{3.24} \begin{cases} \geq 0 \\ \leq 1 \end{cases}, \text{ for SS and CS}$$

$$\mu_{2,punch} = 0.01754 \cdot (b_{slab} / l_{load})^{1.60} \begin{cases} \geq 0 \\ \leq 1 \end{cases}, \text{ for CT} \quad (12)$$

$v_{c,punch,eff}$ considers the influence of self-weight over the shear stresses on the critical perimeter⁵⁵ in the span direction. This study assumes that in one-way slabs, the self-weight acts only in the span direction and hence, it solely affects the shear stresses from the critical perimeter in the slab width direction⁵⁵ ($b_{0,x1}$ and $b_{0,x2}$). Therefore, the distributed loads from the self-weight (v_{sw}) are subtracted from the calculated unitary punching capacity ($v_{c,punch}$) in the corresponding edges from the critical perimeter (perpendicular to the shear span)

$$v_{c,punch,eff} = v_{c,punch} - v_{sw} \quad (13)$$

However, for the small-scale experimental slabs evaluated in this study, the effect of considering $v_{c,punch,eff}$ is negligible.

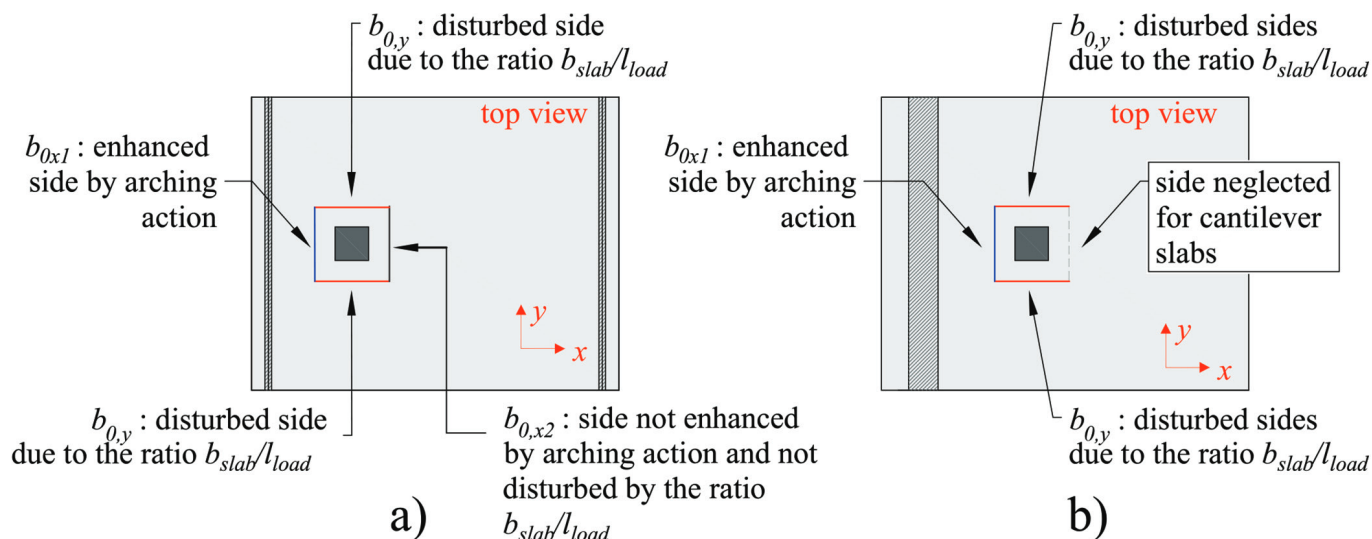


Fig. 11—Sides enhanced or disturbed due to ratio a_v/d_l and b_{slab}/l_{load} : (a) simply supported or continuous slabs; and (b) cantilever slabs.

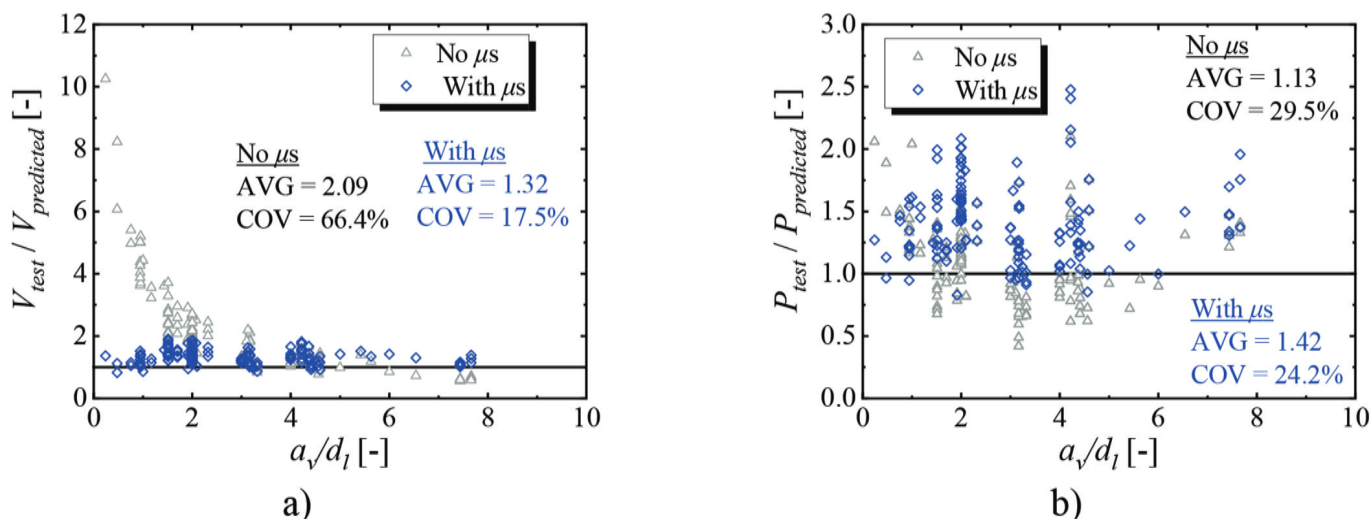


Fig. 12—Comparison between experimental and predicted resistances with ACI expressions with and without correction factors (μ) for: (a) one-way shear according to ratio a_v/d_l ; and (b) punching shear according to ratio a_v/d_l .

RESULTS

Figure 12 shows the relation between experimental and predicted resistances with the shear and punching expressions from ACI 318-19¹⁹ to Database B. Using the proposed correction factors (μ_1 and μ_2) to estimate the sectional shear capacity $V_{predicted}$ improved the accuracy considerably (Fig. 12(a)). The average ratio $V_{test}/V_{predicted}$ changed from 2.09 with a coefficient of variation of 66.4% to an average ratio equal to 1.32 with a coefficient of variation equal to 17.5% (similar to the statistics from the one-way shear expressions applied to members loaded over the entire width⁴⁹). The average ratio $P_{test}/P_{predicted}$ changed from 1.13 with a coefficient of variation of 29.5% to an average ratio of 1.42 with a coefficient of variation of 24.2% using the proposed factors. Therefore, both approaches led to improved levels of accuracy and precision, regardless of the governing failure mechanism.

DISCUSSIONS

Many publications related to one-way slabs under concentrated loads focus on evaluating only one of the possible shear failure mechanisms: the one-way shear failure as wide beams.^{9,18,34,35} Despite most of the tests being rated as failing in this way, looking at only one failure mechanism can induce some bias in the interpretations of test results and limit the understanding of the problem. Punching failures are frequently most critical when the shear slenderness $a_v/d_l > 5$ (Fig. 9(a)) and the ratio $b_{slab}/l_{load} > 12$ (Fig. 9(b)). Therefore, this study tries to provide a most comprehensive look at the problem and warns that both one-way shear and punching shear failure mechanisms shall be discussed for such kinds of slabs. At this point, it is not critical to know from which value of a_v/d_l , for instance, which failure mechanism governs, because both failure mechanisms shall be evaluated in design. Nevertheless, design approaches must consider that the governing failure mechanism and ultimate capacity can vary according to these parameters.

The detailed evaluation of the cracking pattern of one-way slabs under concentrated loads allowed the authors to identify the parameters that influence the transition between one-way shear and two-way shear failure modes. These parameters were mainly the shear slenderness a_v/d_l and the slab width-load size ratio b_{slab}/l_{load} . The effective depth (d_l), the load eccentricity a/l_{span} , as well as the transverse reinforcement ratio ρ_t (refer to Appendix B) also lead to changes in the tested loads (V_{test} and P_{test}) and failure mode. However, the results did not follow a homogeneous behavior by varying the last parameter (ρ_t), so further research is necessary.

Previously, other studies demonstrated experimentally that for the case of slabs subjected to concentrated loads, there is a limiting width b_{slab} after which no further increase in maximum load occurs for increasing width.^{10,14,46} However, the cause for the transition of the failure mode from one-way shear to punching was unclear. This study demonstrated by identifying the failure mechanisms of such slabs that punching failures tend to become more critical by increasing the b_{slab}/l_{load} . Consequently, a higher one-way shear capacity cannot be achieved if the test fails prematurely by punching. Moreover, it was shown that the b_{slab}/l_{load} for which the punching capacity becomes the weakest failure mechanism depends on the slab thickness. In this way, it is reasonable that most approaches for defining the effective shear width^{14,53,54} do not predict a higher contributing width by increasing the slab width after a certain value of b_{slab} .

Most approaches in the literature predict that the effective shear width increases as the shear slenderness a_v/d_l increases.^{12,53} If the shear slenderness is not considered in the unitary shear capacity expressions v_c , the sectional shear capacities V_c will increase for increasing values of the shear slenderness a_v/d_l . As first demonstrated by Reißer,¹⁰ this study also found a predominant tendency to decrease the shear capacity V_{Fu} by increasing the shear slenderness (Fig. 6(a)). However, if one considers a decrease in the unitary shear resistance for increasing values of the shear slenderness a_v/d_l ,^{6,25} such as performed by Natário⁹ using the Critical Shear Crack Theory expressions,²⁵ then it can be demonstrated that the effective shear width increases with the shear slenderness until certain limits. Because the ACI 318-19 code does not include the influence of the shear slenderness parameters in the shear and punching expressions, it is more adequate to consider the effective shear width increases only until a certain point, usually within the region where arching action can favor the load transfer. After a certain value of a_v/d_l , the effective shear width should decrease to avoid unsafe predictions of sectional shear capacity for slabs critical in punching.

Figure 12 shows that both one-way shear and punching shear expressions from the current ACI code can provide satisfactory predictions of the capacity when using appropriate approaches to define the effective shear width and the punching perimeter. However, it can be noted that the predictions of the sectional shear capacity ($V_{test}/V_{predicted}$) are more accurate and precise than the respective punching shear approach. In practice, this occurs because most tests failed as wide beams in one-way shear. The punching failures occurred only locally around the load on the front side of the

load and differed from concentric punching failures. Consequently, the approach based on the sectional shear capacity (which is based on the assumption of a local failure between the load and the support) is more consistent. In theory, the punching shear approach can also be calibrated to reach the same level of accuracy as the one-way shear approach. However, to achieve this, it would be necessary to include more parameters in the punching shear approach, such as the effective depth d_{avg} and the load eccentricity a/l_{span} . In this study, only two main parameters for both approaches are proposed for simplicity.

CONCLUSIONS

One-way slabs under concentrated loads may fail by one-way shear (as wide beams), punching shear, or a mixed failure mode between them. In the literature, the test results were frequently addressed by evaluating only the one-way shear failure mechanism^{9,18,34,35} or the punching shear mechanism.⁵⁶ Therefore, the understanding of the problem was commonly discussed using a narrower background. In this study, the main characteristics of the one-way and two-way shear failure mechanisms were reviewed and discussed to allow a broader insight into the mechanics of the problem. Besides, comparative analyses were carried out using the ACI 318-19 code expressions with most traditional design rules to verify the sectional shear capacity and punching capacity of a database of test results. An enhanced approach to define the effective shear width and the effective shear resisting control perimeter was proposed. From this study, the following conclusions can be drawn:

- Different shear failure mechanisms may occur according to parameters such as the shear slenderness a_v/d_l , slab width-load size ratio b_{slab}/l_{load} , and transverse reinforcement ratio ρ_t . The authors identified that the first two are the most important parameters influencing the transition from one-way to two-way shear failure.
- From the literature review and by bringing together test results from several references, it was identified that: 1) both shear and punching failure modes may occur for $a_v/d_l < 3$, but punching failures are most frequently the governing failure mechanism for $a_v/d_l > 5$; 2) the tested shear capacity V_{test} of slabs under concentrated loads usually does not increase by increasing the shear slenderness a_v/d_l ; and 3) punching is the governing failure mechanism for one-way slabs with $b_{slab}/l_{load} > 12$.
- The ultimate capacity of one-way slabs under concentrated loads increases only until a certain limit by increasing the ratio b_{slab}/l_{load} . This behavior occurs because there is an upper limit for the effective shear width, as verified by other authors,^{35,36} and also because punching failure becomes the governing failure mechanism for slabs after a specific value of b_{slab}/l_{load} .
- While the transverse reinforcement ratio plays a marked influence on the cracking pattern and transverse distribution of shear forces on the slab width, uniform conclusions on the effect of this parameter could not be formulated. Therefore, further experiments are required to study the influence of the transverse reinforcement ratio on the transition between shear and punching failures.

- The proposed correction factor ($\mu_{1,shear}$) to account for the enhanced shear capacity of slabs under concentrated loads close to the support improved the precision of the one-way shear expressions from ACI 318-19 significantly without the need for complex three-dimensional strut-and-tie models or finite element analyses. Moreover, the second factor related to the shear slenderness a_v/d_l ($\mu_{2,shear}$) improves the predictions of the sectional shear capacity $V_{predicted}$ for tests that may be critical in punching. In this way, safe and accurate predictions of shear capacity can be achieved using only the one-way shear expressions, regardless of the most critical failure mechanism of the slabs.

In summary, the design and assessment of one-way slabs under concentrated loads must consider that shear and punching failure modes can occur. Moreover, the evaluation of test results from the literature needs to be carried out more comprehensively by studying the governing shear failure mechanism, evaluating the corresponding sectional shear and failure loads, and linking these observations to the distribution of shear stresses around the load and near the support so that the mechanics of the problem can be better understood.

AUTHOR BIOS

Alex M. D. de Sousa is a Postdoctoral Fellow at the São Carlos School of Engineering (EESC) at the University of São Paulo (USP), São Carlos, Brazil. His research interests include the shear, punching, and numerical modeling of reinforced concrete structures.

ACI member Eva O. L. Lantsoght is a Full Professor at Universidad San Francisco de Quito, Quito, Ecuador, and an Assistant Professor at Delft University of Technology, Delft, the Netherlands. She is the Vice-Chair of Joint ACI-ASCE Subcommittee 445-E, SOA Torsion; Secretary of Joint ACI-ASCE Committee 421, Design of Reinforced Concrete Slabs; and a member of ACI Committees 342, Evaluation of Concrete Bridges and Bridge Elements, and 437, Strength Evaluation of Existing Concrete Structures; Joint ACI-ASCE Committee 445, Shear and Torsion; and Joint ACI-ASCE Subcommittee 445-D, Shear Databases.

Mounir K. El Debs is a Senior Professor at EESC-USP, where he received his MSc and PhD in structural engineering in 1976 and 1984, respectively. His research interests include reinforced and prestressed concrete, precast concrete, and thin-walled concrete elements.

ACKNOWLEDGMENTS

The authors acknowledge the financial support provided by the Brazilian National Council for Scientific and Technological Development (CNPq) (grant number 303438/2016-9) and the São Paulo Research Foundation (FAPESP) (grant numbers 2018/21573-2, 2019/20092-3, and 2021/13916-0).

REFERENCES

1. Lantsoght, E. O. L.; van der Veen, C.; de Boer, A.; and Walraven, J. C., "Transition from One-Way to Two-Way Shear in Slabs under Concentrated Loads," *Magazine of Concrete Research*, V. 67, No. 17, 2015, pp. 909-922. doi: 10.1680/mac.14.00124
2. Lantsoght, E. O. L.; van der Veen, C.; and Walraven, J. C., "Shear in One-Way Slabs under Concentrated Load Close to Support," *ACI Structural Journal*, V. 110, No. 2, Mar.-Apr. 2013, pp. 275-284.
3. Tenório, D. A.; Gomes, P. C. C.; Désir, J. M.; and Uchôa, E. L. M., "Analysis of Accidental Loads on Garage Floors," *Revista IBRACON de Estruturas e Materiais*, V. 7, No. 4, 2014, pp. 560-571.
4. Bui, T. T.; Limam, A.; Nana, W.-S.-A.; Ferrier, E.; Bost, M.; and Bui, Q.-B., "Evaluation of One-Way Shear Behaviour of Reinforced Concrete Slabs: Experimental and Numerical Analysis," *European Journal of Environmental and Civil Engineering*, V. 24, No. 2, 2020, pp. 190-216. doi: 10.1080/19648189.2017.1371646
5. Bui, T. T.; Abouri, S.; Limam, A.; Nana, W.-S.-A.; Tedoldi, B.; and Roure, T., "Experimental Investigation of Shear Strength of Full-Scale Concrete Slabs Subjected to Concentrated Loads in Nuclear Buildings," *Engineering Structures*, V. 131, 2017, pp. 405-420. doi: 10.1016/j.engstruct.2016.10.045
6. de Sousa, A. M. D.; Lantsoght, E. O. L.; and El Debs, M. K., "One-Way Shear Strength of Wide Reinforced Concrete Members without Stirrups," *Structural Concrete*, V. 22, No. 2, 2021, pp. 968-992. doi: 10.1002/suco.202000034
7. Reineck, K.-H.; Bentz, E. C.; Fitik, B.; Kuchma, D. A.; and Bayrak, O., "ACI-DAFStb Database of Shear Tests on Slender Reinforced Concrete Beams without Stirrups," *ACI Structural Journal*, V. 110, No. 5, Sept.-Oct. 2013, pp. 867-876.
8. Muttoni, A., "Punching Shear Strength of Reinforced Concrete Slabs without Transverse Reinforcement," *ACI Structural Journal*, V. 105, No. 4, July-Aug. 2008, pp. 440-450.
9. Natário, F.; Fernández Ruiz, M.; and Muttoni, A., "Shear Strength of RC Slabs under Concentrated Loads Near Clamped Linear Supports," *Engineering Structures*, V. 76, 2014, pp. 10-23. doi: 10.1016/j.engstruct.2014.06.036
10. Reiß, K., "Zum Querkrafttragverhalten von einachsig gespannten Stahlbetonplatten ohne Querkraftbewehrung unter Einzellasten," PhD thesis, Faculty of Civil Engineering, RWTH Aachen University, Aachen, Germany, 2016.
11. Lantsoght, E. O. L.; van der Veen, C.; Walraven, J. C.; and de Boer, A., "Database of Wide Concrete Members Failing in Shear," *Magazine of Concrete Research*, V. 67, No. 1, 2015, pp. 33-52. doi: 10.1680/mac.14.00137
12. NF EN, 1992, "Eurocode 2 - Calcul des structures en béton - Guide d'application des normes," European Committee for Standardization, Brussels, Belgium, 2013.
13. Regan, P. E., "Shear Resistance of Concrete Slabs at Concentrated Loads Close to Supports," Polytechnic of Central London, London, UK, 1982.
14. Lantsoght, E. O. L., "Shear in Reinforced Concrete Slabs under Concentrated Loads Close to Supports," PhD thesis, Faculty of Civil Engineering and Geosciences, Delft University of Technology, Delft, the Netherlands, 2013.
15. Reiß, K., and Hegger, J., "Database of Shear Tests on RC Slabs without Shear Reinforcement under Concentrated Loads - Assessment of Design Rules According to Eurocode 2," 16th European Bridge Conference, Edinburgh, UK, 2015.
16. Sousa, A. M. D., and El Debs, M. K., "Shear Strength Analysis of Slabs without Transverse Reinforcement under Concentrated Loads According to ABNT NBR 6118:2014," *IBRACON Structures and Materials Journal*, V. 12, No. 3, 2019, pp. 658-693. doi: 10.1590/s1983-41952019000300012
17. EN 1992-1-1:2005, "Eurocode 2: Design of Concrete Structures — Part 1-1: General Rules and Rules for Buildings," European Committee for Standardization, Brussels, Belgium, 2005.
18. Halvonik, J.; Vidaković, A.; and Vida, R., "Shear Capacity of Clamped Deck Slabs Subjected to a Concentrated Load," *Journal of Bridge Engineering*, ASCE, V. 25, No. 7, 2020, p. 04020037. doi: 10.1061/(ASCE)BE.1943-5592.0001564
19. ACI Committee 318, "Building Code Requirements for Structural Concrete (ACI 318-19) and Commentary (ACI 318R-19)," American Concrete Institute, Farmington Hills, MI, 2019, 623 pp.
20. Mörsch, E., *Der Eisenbetonbau [Concrete-Steel Construction]*, Engineering News Publishing, New York, 1909.
21. Walraven, J. C., "Fundamental Analysis of Aggregate Interlock," *Journal of the Structural Division*, ASCE, V. 107, No. 11, 1981, pp. 2245-2270. doi: 10.1061/JSDEAG.0005820
22. Taylor, H. P., "Investigation of the Dowel Shear Forces Carried by the Tensile Steel in Reinforced Concrete Beams," Tech Rept TRA 431, Cement and Concrete Association, London, UK, 1969, 24 pp.
23. Hordijk, D. A., "Tensile and Tensile Fatigue Behaviour of Concrete — Experiments, Modelling and Analyses," *Heron*, V. 37, No. 1, 1992, pp. 3-79.
24. Kani, G. N. J., "The Riddle of Shear Failure and its Solution," *ACI Journal Proceedings*, V. 61, No. 4, Apr. 1964, pp. 441-468.
25. Muttoni, A., and Ruiz, M. F., "Shear Strength of Members without Transverse Reinforcement as Function of Critical Shear Crack Width," *ACI Structural Journal*, V. 105, No. 2, Mar.-Apr. 2008, pp. 163-172.
26. Muttoni, A., and Ruiz, M. F., "Shear in Slabs and Beams: Should They be Treated in the Same Way?" *fib Bulletin*, N°57, Fédération Internationale du Béton, Lausanne, Switzerland, 2010, pp. 105-128.
27. Mari, A.; Cladera, A.; Oller, E.; and Bairán, J. M., "A Punching Shear Mechanical Model for Reinforced Concrete Flat Slabs with and without Shear Reinforcement," *Engineering Structures*, V. 166, 2018, pp. 413-426. doi: 10.1016/j.engstruct.2018.03.079

28. Cavagnis, F.; Fernández Ruiz, M.; and Muttoni, A., "A Mechanical Model for Failures in Shear of Members without Transverse Reinforcement Based on Development of a Critical Shear Crack," *Engineering Structures*, V. 157, 2018, pp. 300-315. doi: 10.1016/j.engstruct.2017.12.004
29. Criswell, M. E., and Hawkins, N. W., "Shear Strength of Slabs: Basic Principle and Their Relation to Current Methods of Analysis," *Shear in Reinforced Concrete - Volume 1 and 2*, American Concrete Institute, Farmington Hills, MI, 1974, pp. 641-676.
30. Hawkins, N. M., and Mitchell, D., "Progressive Collapse of Flat Plate Structures," *ACI Journal Proceedings*, V. 76, No. 7, July 1979, pp. 775-808.
31. Menétrey, P., "Synthesis of Punching Failure in Reinforced Concrete," *Cement and Concrete Composites*, V. 24, No. 6, 2002, pp. 497-507. doi: 10.1016/S0958-9465(01)00066-X
32. Yang, Y.; den Uijl, J.; and Walraven, J., "Critical Shear Displacement Theory: On the Way to Extending the Scope of Shear Design and Assessment for Members without Shear Reinforcement," *Structural Concrete*, V. 17, No. 5, 2016, pp. 790-798. doi: 10.1002/suco.201500135
33. Doorgeest, J., "Transition Between One-way Shear and Punching Shear," MS thesis, Delft University of Technology, Delft, the Netherlands, 2012.
34. Henze, L.; Rombach, G. A.; and Harter, M., "New Approach for Shear Design of Reinforced Concrete Slabs under Concentrated Loads Based on Tests and Statistical Analysis," *Engineering Structures*, V. 219, 2020, p. 110795. doi: 10.1016/j.engstruct.2020.110795
35. Reiß, K.; Classen, M.; and Hegger, J., "Shear in Reinforced Concrete Slabs-Experimental Investigations in the Effective Shear Width of One-Way Slabs under Concentrated Loads and with Different Degrees of Rotational Restraint," *Structural Concrete*, V. 19, No. 1, 2018, pp. 36-48. doi: 10.1002/suco.201700067
36. Lantsoght, E. O. L.; van der Veen, C.; de Boer, A.; and Walraven, J. C., "Influence of Width on Shear Capacity of Reinforced Concrete Members," *ACI Structural Journal*, V. 111, No. 6, Nov.-Dec. 2014, pp. 1441-1449. doi: 10.14359/51687107
37. de Sousa, A.; Lantsoght, E.; Setiawan, A.; and El Debs, M. K., "Transition from One-Way to Two-Way Shear by Coupling LEFEA and the CSCT Models," *Proceedings of the fib Symposium 2021, Concrete Structures: New Trends for Eco-Efficiency and Performance*, 2021.
38. Henze, L., "Querkrafttragverhalten von Stahlbeton-Fahrbahnplatten," PhD thesis, Institute for Concrete Structures, Technische Universität Hamburg, Hamburg, Germany, 2019.
39. Sagaseta, J., and Vollum, R. L., "Influence of Aggregate Fracture on Shear Transfer through Cracks in Reinforced Concrete," *Magazine of Concrete Research*, V. 63, No. 2, 2011, pp. 119-137. doi: 10.1680/mac.9.00191
40. Sagaseta, J.; Tassinari, L.; Fernández Ruiz, M.; and Muttoni, A., "Punching of Flat Slabs Supported on Rectangular Columns," *Engineering Structures*, V. 77, 2014, pp. 17-33. doi: 10.1016/j.engstruct.2014.07.007
41. Natário, F., "Static and Fatigue Shear Strength of Reinforced Concrete Slabs Under Concentrated Loads Near Linear Support," PhD thesis, École Polytechnique Fédérale de Lausanne, Lausanne, Switzerland, 2015.
42. de Sousa, A. M. D.; Lantsoght, E. O. L.; and El Debs, M. K., "Databases of One-Way Slabs under Concentrated Loads: Parameter Analyses and Validation of the Proposed Approach," 2022, <https://zenodo.org/record/5911469>. (last accessed Jan. 20, 2023)
43. Rombach, G., and Henze, L., "Querkrafttragfähigkeit von Stahlbetonplatten ohne Querkraftbewehrung unter konzentrierten Einzellasten," *Beton- und Stahlbetonbau*, V. 112, No. 9, 2017, pp. 568-578. doi: 10.1002/best.201700040
44. Cullington, D. W.; Daly, A. F.; and Hill, M. E., "Assessment of Reinforced Concrete Bridges: Collapse Tests on Thurloxton Underpass," *Bridge Management*, V. 3, 1996, pp. 667-674.
45. Ferreira, M. P., "Experimental Analysis of One-Way Reinforced Concrete Flat Slabs in Axis or Non-Axis-Symmetric Punching Shear," doctoral thesis, Universidade Federal do Pará, Belém, Brazil, 2006.
46. Regan, P. E., and Rezai-Jorabi, H., "Shear Resistance of One-Way Slabs Under Concentrated Loads," *ACI Structural Journal*, V. 85, No. 2, Mar.-Apr. 1988, pp. 150-157.
47. Damasceno, L. S. R., "Experimental Analysis of One-Way Reinforced Concrete Flat Slabs in Punching Shear with Rectangular Columns," master's dissertation, Departamento de Engenharia Civil, Universidade Federal do Pará, Belém, Brazil, 2007.
48. Belarbi, A.; Kuchma, D. A.; and Sanders, D. H., "Proposals for New One-Way Shear for the 318 Building Code," *Concrete International*, V. 39, No. 9, Sept. 2017, pp. 29-32.
49. Kuchma, D. A.; Wei, S.; Sanders, D. H.; Belarbi, A.; and Novak, L. C., "Development of One-Way Shear Design Provisions of ACI 318-19 for Reinforced Concrete," *ACI Structural Journal*, V. 116, No. 4, July 2019, pp. 285-295. doi: 10.14359/51716739
50. Lantsoght, E. O. L.; van der Veen, C.; Walraven, J.; and de Boer, A., "Experimental Investigation on Shear Capacity of Reinforced Concrete Slabs with Plain Bars and Slabs on Elastomeric Bearings," *Engineering Structures*, V. 103, 2015, pp. 1-14. doi: 10.1016/j.engstruct.2015.08.028
51. Widiyanto; Bayrak, O.; and Jirsa, J. O., "Two-Way Shear Strength of Slab-Column Connections: Reexamination of ACI 318 Provisions," *ACI Structural Journal*, V. 106, No. 2, Mar.-Apr. 2009, pp. 160-170.
52. Regan, P. E., "Shear Resistance of Members without Shear Reinforcement," *Proposal for CEB Model Code*, V. MC90, 1987, pp. 1-28.
53. *fib*, "fib Model Code for Concrete Structures 2010," V. 1-2, *fédération internationale du béton*, Lausanne, Switzerland, 2012.
54. de Sousa, A. M. D.; Lantsoght, E. O. L.; Yang, Y.; and El Debs, M. K., "Extended CSCT Model for Shear Capacity Assessments of Bridge Deck Slabs," *Engineering Structures*, V. 234, 2021, p. 111897. doi: 10.1016/j.engstruct.2021.111897
55. Lantsoght, E. O. L.; van der Veen, C.; de Boer, A.; and Alexander, S. D. B., "Bridging the Gap between One-Way and Two-Way Shear in Slabs," *ACI-fib International Symposium: Punching Shear of Structural Concrete Slabs*, SP-315, American Concrete Institute, Farmington Hills, MI, 2017, pp. 187-214.
56. Vaz Rodrigues, R.; Fernández Ruiz, M.; and Muttoni, A., "Shear Strength of R/C Bridge Cantilever Slabs," *Engineering Structures*, V. 30, No. 11, 2008, pp. 3024-3033. doi: 10.1016/j.engstruct.2008.04.017

Appendix A. GPR maps with variable scanning rates

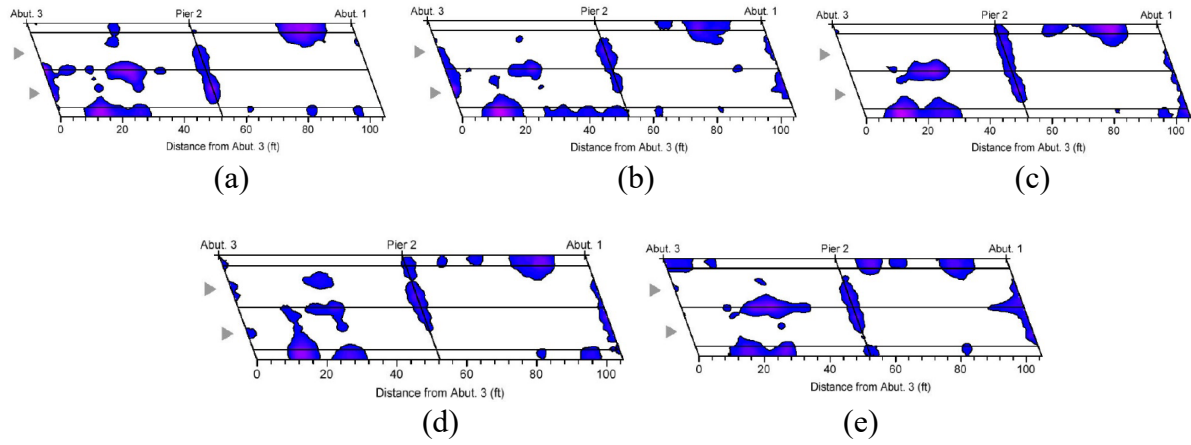


Fig. A1. B06A: (a) 4 scans/ft; (b) 8 scans/ft; (c) 12 scans/ft; (d) 16 scans/ft; (e) 20 scans/ft

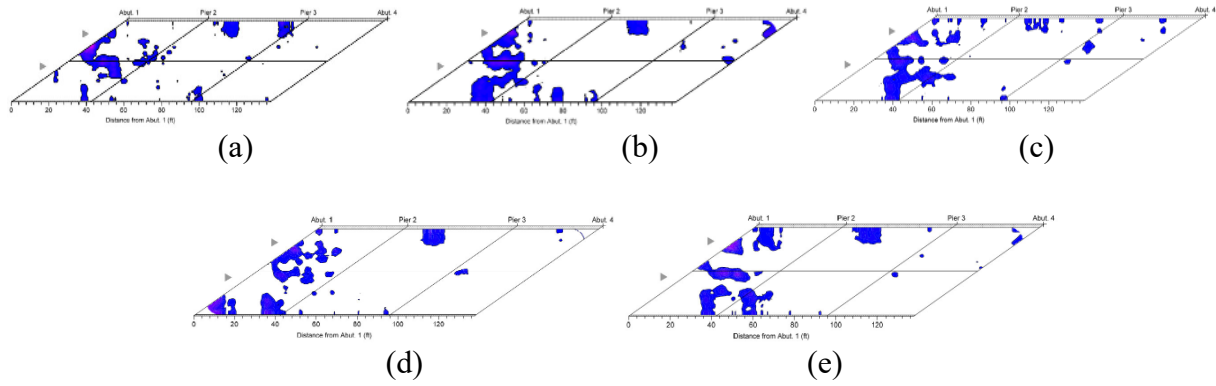


Fig. A2. B06S: (a) 4 scans/ft; (b) 8 scans/ft; (c) 12 scans/ft; (d) 16 scans/ft; (e) 20 scans/ft

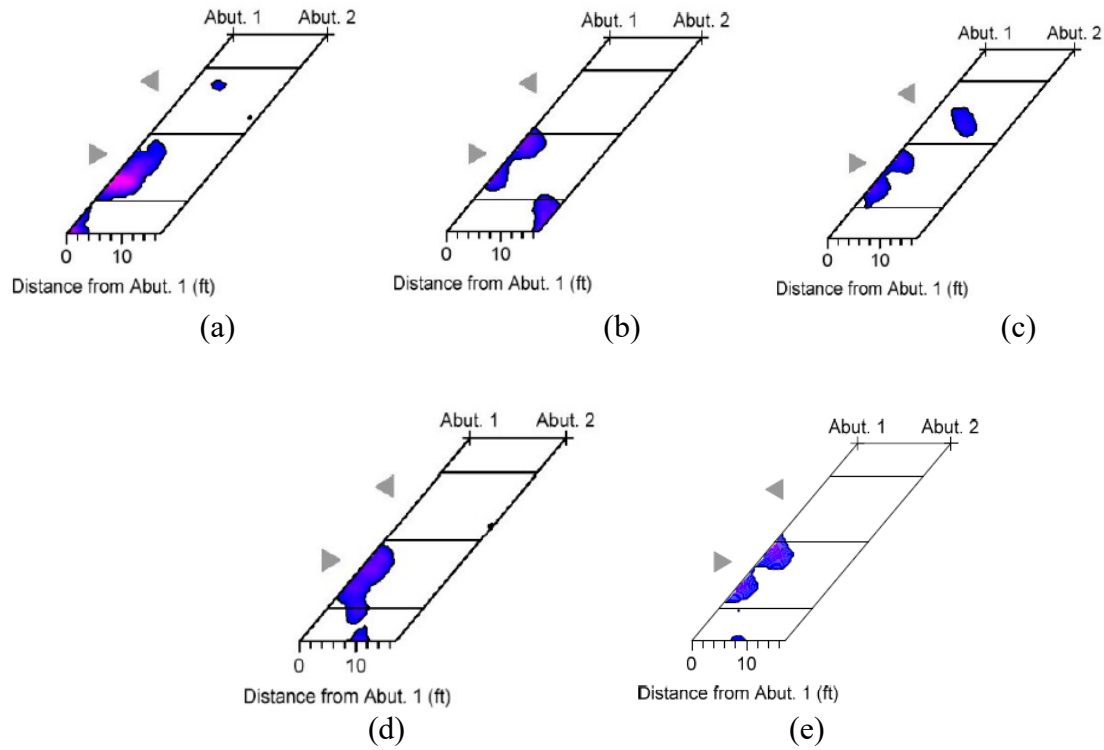


Fig. A3. C08A: (a) 4 scans/ft; (b) 8 scans/ft; (c) 12 scans/ft; (d) 16 scans/ft; (e) 20 scans/ft

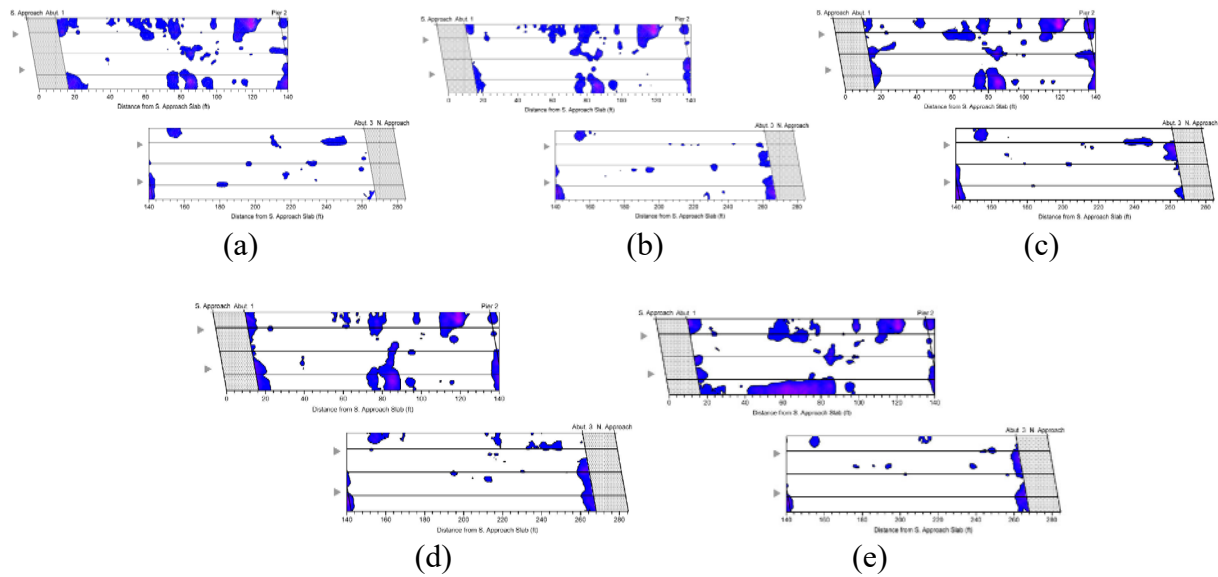


Fig. A4. B06V: (a) 4 scans/ft; (b) 8 scans/ft; (c) 12 scans/ft; (d) 16 scans/ft; (e) 20 scans/ft

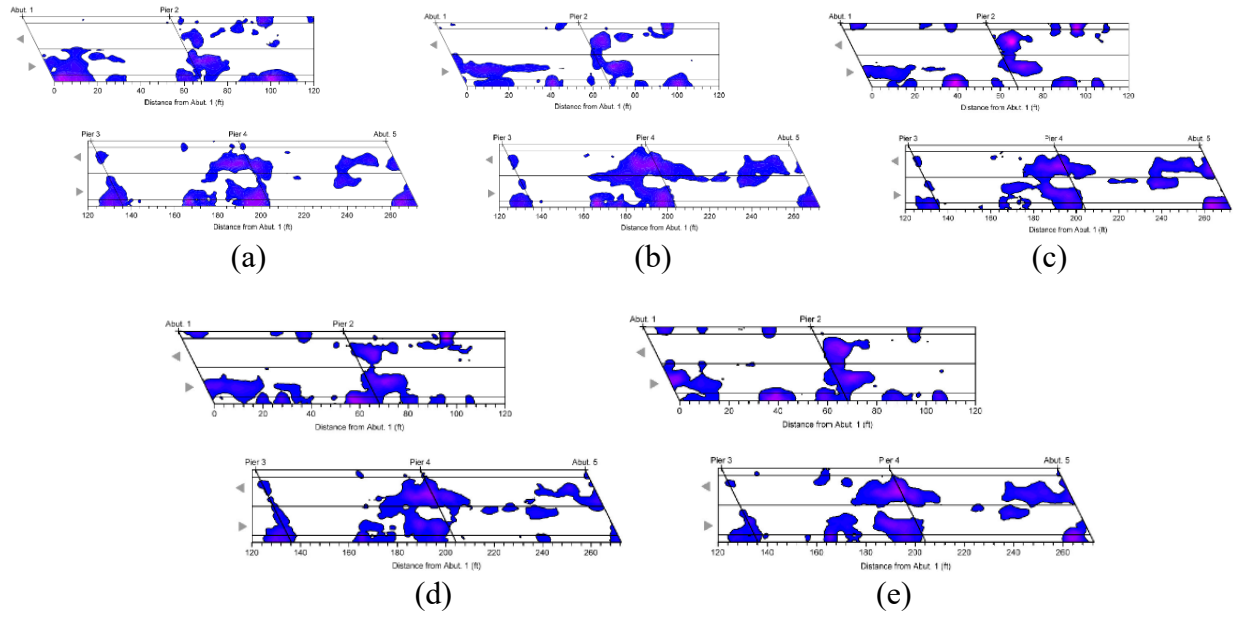


Fig. A5. C07A: (a) 4 scans/ft; (b) 8 scans/ft; (c) 12 scans/ft; (d) 16 scans/ft; (e) 20 scans/ft

